J Math Chem (2015) 53:386–401
DOI 10.1007/s10910-014-0430-1

ORIGINAL PAPER

Effects of reaction reversibility on ignition and flame propagation

Cong Li · Yunchao Wu · Zheng Chen

Received: 13 September 2014 / Accepted: 6 October 2014 / Published online: 17 October 2014

Abstract Chemical reactions in high-temperature combustion are reversible and reaction reversibility might have a great impact on fundamental combustion processes such as ignition and flame propagation. In this study, ignition and propagation of spherical flames with a reversible reaction are analyzed using the large-activation-energy asymptotic method. Analytical correlations are derived to describe the change of spherical flame propagation speed and flame temperature with flame radius. The reversibility parameter, fuel Lewis number, and ignition power are included in these correlations. These correlations can predict different flame regimes and transitions among the ignition kernel, flame ball, propagating spherical flame, and planar flame. Therefore, based on these correlations spherical flame propagation and initiation are then investigated with the emphasis on assessing the impact of reaction reversibility. It is found that

Electronic supplementary material The online version of this article (doi:10.1007/s10910-014-0430-1) contains supplementary material, which is available to authorized users.

C. Li · Y. Wu · Z. Chen (✉)
State Key Laboratory for Turbulence and Complex Systems (SKLTCS), Department of Mechanics and Engineering Science, College of Engineering, Peking University, Room 408, Beijing 100871, China
e-mail: cz@pku.edu.cn

C. Li
e-mail: licong199159@pku.edu.cn

Y. Wu
e-mail: wuyunchaojiangsu@vip.qq.com

Z. Chen
Department of Aeronautics and Astronautics, College of Engineering, Peking University, Beijing 100871, China

Present address:
C. Li · Y. Wu
Department of Mechanical Engineering, University of Connecticut, Storrs, CT, USA

similar to heat loss, reaction reversibility can greatly affect spherical flame propagation speed, Markstein length, flame ball radius, minimum ignition power, and critical ignition radius. Moreover, it is demonstrated that the influence of reaction reversibility depends on fuel Lewis number.

Keywords Ignition · Spherical flame propagation · Reversible reaction · Markstein length · Lewis number

1 Introduction

Ignition and flame propagation are two of the most fundamental combustion problems. They are related to fire safety control and development of advance internal combustion engines and thereby receive great attention in combustion community. Due to its simple geometry, ignition and propagation of spherical flame have been extensively studied via theoretical analysis [1–11], numerical simulation [12–15], and experiments [1,16–18] (see also references in [19]).

In theoretical studies on spherical flame initiation and propagation (e.g. [1–11]), one-step, irreversible reaction of the form F $\rightarrow$ P was employed. In such a one-step model, fuel (denoted by F) is converted directly into products (denoted by P) and heat. Consequently, the role of reaction reversibility as well as energetic active radicals is not considered in these studies. In practical combustion of hydrocarbon fuels, reversible elementary reactions related to fuel and intermediate species (radicals) always appear. As such, it is expected that ignition and flame propagation are affected by reaction reversibility and properties of radicals involved in chain branching reactions.

Recently, Zhang et al. [20,21] have analyzed the spherical flame initiation and propagation considering the thermally sensitive intermediate kinetics, which includes a chain-branching reaction and a recombination reaction [22]. It has been found that the spherical flame propagation speed, Markstein length, and critical ignition conditions are all affected by the transport and chemical properties of radicals involved in the chain reactions [20,21]. This two-step chain-branching model was also used in previous studies on propagation, extinction, and stability of premixed flames [23–30]. In these studies [20–30] as well as previous studies considering one-step chemistry [1–11], the irreversible reaction model was employed and thereby the influence of reaction reversibility on ignition and propagation of spherical flame was not addressed.

As pointed out by Daou [31–33], the reaction reversibility is a fundamental realistic aspect in combustion and it might have a great impact on fundamental combustion phenomena. Daou analyzed the influence of reaction reversibility on premixed planar flame [31], triple flame [32], and premixed counterflow flame [33] using a one-step reversible reaction model. It was found that reaction reversibility can greatly affect fundamental combustion properties such as flame propagation speed and quenching limit. However, to the authors' knowledge, the influence of reverse reaction on ignition has not been investigated. In spark ignition process, the temperature inside the ignition kernel after spark discharge is usually very high, indicating that there exists pronounced reversibility of chemical reactions (global or elementary). Usually the forward reaction, F $\rightarrow$ P, is exothermic; while the backward reaction, F $\leftarrow$ P, is endothermic. With the increase of the reaction reversibility, the combustion intensity and flame temperature both decrease [31–33]. As a result, it is expected that the critical ignition conditions are strongly influenced by the reaction reversibility.

The objectives of this study are therefore to provide a theoretical description of spherical flame initiation and propagation with a reversible reaction and to analytically assess the influence of reaction reversibility. The emphasis is placed on examining how the spherical flame propagation speed, Markstein length, and critical ignition condition are affected by the reverse reaction. The rest of the paper is organized as follows. The mathematical model and analytical solutions are presented the next section. In Sect. 3, the effects of reaction reversibility on spherical flame propagation and ignition is examined. Finally, the conclusions are summarized in Sect. 4.

2 Theoretical analysis

2.1 Mathematical model

We consider one-dimensional, adiabatic, premixed, spherical flame initiation and propagation. In order to include reaction reversibility, a single reversible reaction in the form of F $\Leftrightarrow$ P is considered. The mathematical model is similar to that in Ref. [10] and thereby it is only briefly described below. The readers are referred to the Supplementary Document in which details on governing equations and their reduction and non-dimensionalization are provided.

The constant density and quasi-steady assumptions [6–9] are employed. In the coordinate attached to the propagating flame front, the non-dimensional governing equations for temperature, T, and mass fractions of fuel, Y_F, and product, Y_P, are

$$-U\frac{dT}{d\xi} = \frac{1}{(\xi+R)^2}\frac{d}{d\xi}\left[(\xi+R)^2\frac{dT}{d\xi}\right] + \omega \tag{1a}$$

$$-U\frac{dY_F}{d\xi} = \frac{Le_F^{-1}}{(\xi+R)^2}\frac{d}{d\xi}\left[(\xi+R)^2\frac{dY_F}{d\xi}\right] - \omega \tag{1b}$$

$$-U\frac{dY_P}{d\xi} = \frac{Le_P^{-1}}{(\xi+R)^2}\frac{d}{d\xi}\left[(\xi+R)^2\frac{dY_P}{d\xi}\right] + \omega \tag{1c}$$

where ξ is the non-dimensional radial coordinate; R is the flame radius; Le_F and Le_Z are the Lewis numbers of the fuel and radical, respectively; and U is the non-dimensional flame propagation speed (normalized by the adiabatic planar flame speed for the irreversible case).

The non-dimensional reaction rate in the above governing equations is

$$\omega = \frac{Z_{ad}^2}{2Le_F}\left\{Y_F\exp\left[\frac{Z_{ad}(T-1)}{\sigma+(1-\sigma)T}\right] - \Gamma Y_P\exp\left[\frac{Z_{ad}[T(1-\sigma)+\sigma-\Theta]}{(1-\sigma)[\sigma+(1-\sigma)T]}\right]\right\} \tag{2}$$

in which Z_{ad} is the Zel'dovich number and σ is the temperature ratio between unburned and burned gases. Both Z_{ad} and σ are defined under the irreversible condition. Γ and Θ are respectively the ratios of the pre-exponential factors and activation energies of the backward and forward reactions. For the irreversible condition, we have $\Gamma = 0$ (i.e. only the forward reaction happens). Similar to the work of Daou [31], the variable Γ is the main parameter in this study and it is referred to as the reversibility parameter. The difference in the activation energies of the backward and forward reactions is equal to the enthalpy of the reaction in the case of an elementary reaction [31] and thereby we have $\Theta \approx [1 + (1 - \sigma)^2/Z_{ad}]$.

In this study, the ignition power, Q, is provided as a heat flux at the center [7,10] (the limitation on this assumption is discussed in Ref. [10]). The boundary conditions are

$$\xi \to -R : (\xi + R)^2 \frac{dT}{d\xi} = -Q, \frac{dY_F}{d\xi} = 0 \frac{dY_P}{d\xi} = 0 \tag{3a}$$

$$\xi \to \infty : T = 0, Y_F = 1, Y_P = 0 \tag{3b}$$

The above model extends previous analytical description [7,10] of spherical flame initiation and propagation beyond the common framework of a one-step irreversible Arrhenius reaction. The previous analytical description [7,10] is the limiting case of zero reversibility parameter ($\Gamma = 0$) in the present study.

2.2 Analytical solutions

The propagating spherical flame with a reversible reaction is analyzed using the large-activation-energy asymptotic method [2,34]. The flame structure consists of the upstream preheat zone ($\xi > 0$) and downstream equilibrium zone ($-R \leq \xi < 0$), which are connected by the thin reaction zone located around $\xi = 0$. At large activation energy, the ratio between the thickness of the inner reaction zone and that of the outer preheat zone is a small parameter, ε, which is the inverse of the Zel'dovich number (i.e. $\varepsilon = 1/Z_{ad}$) [34]. Following the procedure for asymptotic analysis of planar and spherical flames with a one-step irreversible reaction [34,35], the asymptotic solution is obtained in ascending powers of this small parameter and then asymptotically matched. The details on asymptotic analysis are not repeated here and the readers are referred to the Supplementary Document for the detailed derivation.

From asymptotic analysis, we obtain the following correlations which determine the flame propagation speed, U, and flame temperature, T_b, as functions of flame radius, R:

$$\frac{T_b R^{-2} e^{-UR}}{\int_R^\infty s^{-2} e^{-Us} ds} - QR^{-2} e^{-UR} = \frac{1}{Le_F} \frac{(1 - Y_{F,b}) e^{-URLe_F}}{\int_R^\infty s^{-2} e^{-ULe_F s} ds}$$
$$= \frac{1}{Le_P} \frac{Y_{P,b} e^{-URLe_P}}{\int_R^\infty s^{-2} e^{-ULe_P s} ds} \tag{4}$$

$$
\begin{aligned}
&1 - Le_F\left(\frac{T_b}{\int_R^\infty s^{-2}e^{-Us}ds} - Q\right)\frac{\int_R^\infty s^{-2}e^{-ULe_F s}ds}{e^{-UR(Le_F-1)}}\\
&\quad = \Gamma Le_P\left(\frac{T_b}{\int_R^\infty s^{-2}e^{-Us}ds} - Q\right)\\
&\quad\quad \times \frac{\int_R^\infty s^{-2}e^{-ULe_P s}ds}{e^{-UR(Le_P-1)}}\exp\left[\frac{Z_{ad}(1-\Theta)}{(1-\sigma)[\sigma+(1-\sigma)T_b]}\right]
\end{aligned}
\tag{5}
$$

$$
\begin{aligned}
&\left(\frac{T_b}{\int_R^\infty s^{-2}e^{-Us}ds} - Q\right)R^{-2}e^{-UR} = [\sigma+(1-\sigma)T_b]^2\exp\left[\frac{Z_{ad}}{2}\frac{T_b-1}{\sigma+(1-\sigma)T_b}\right]\\
&\quad \times\sqrt{1+\Gamma\left[\frac{Le_P}{Le_F}-\frac{Y_{P,b}}{Le_F}\frac{Z_{ad}(1-\Theta)}{[\sigma+(1-\sigma)T_b]^2}\right]\exp\left[\frac{Z_{ad}(1-\Theta)}{(1-\sigma)[\sigma+(1-\sigma)T_b]}\right]}
\end{aligned}
\tag{6}
$$

By solving Eqs. (4–6) numerically, the change of flame kernel propagation speed U with flame radius R at different ignition power Q, reversibility parameter Γ, and fuel Lewis number Le_F can be obtained and thereby the ignition and propagation of spherical flames can be investigated.

In the limit of infinite flame radius ($R \to \infty$), Eqs. (4–6) respectively reduce to

$$T_b = 1 - Y_{F,b} = Y_{P,b} \tag{7}$$

$$1 - T_b = \Gamma T_b \exp\left[\frac{Z_{ad}(1-\Theta)}{(1-\sigma)[\sigma+(1-\sigma)T_b]}\right] \tag{8}$$

$$
\begin{aligned}
U &= \frac{[\sigma+(1-\sigma)T_b]^2}{T_b}\exp\left[\frac{Z_{ad}}{2}\frac{T_b-1}{\sigma+(1-\sigma)T_b}\right]\\
&\quad\times\sqrt{1+\Gamma\left[\frac{Le_P}{Le_F}-\frac{Y_{P,b}}{Le_F}\frac{Z_{ad}(1-\Theta)}{[\sigma+(1-\sigma)T_b]^2}\right]\exp\left[\frac{Z_{ad}(1-\Theta)}{(1-\sigma)[\sigma+(1-\sigma)T_b]}\right]}
\end{aligned}
\tag{9}
$$

which are the same as the results for adiabatic planar flame with a reversible reaction derived by Daou [31]. In the limit of irreversible case (i.e. $\Gamma = 0$), Eqs. (4–6) reduce to

$$
\begin{aligned}
\frac{T_b R^{-2}e^{-UR}}{\int_R^\infty s^{-2}e^{-Us}ds} - QR^{-2}e^{-UR} &= \frac{1}{Le_F}\frac{R^{-2}e^{-URLe_F}}{\int_R^\infty s^{-2}e^{-ULe_F s}ds}\\
&= [\sigma+(1-\sigma)T_b]^2\exp\left[\frac{Z_{ad}}{2}\frac{T_b-1}{\sigma+(1-\sigma)T_b}\right]
\end{aligned}
\tag{10}
$$

which are the same as the results for propagating spherical flame in [10,35]. Therefore, the present analysis is consistent with previous studies on adiabatic planar [31] and spherical flames [10,35].

3 Results and discussion

3.1 Effects of reaction reversibility on flame speed and Markstein length

The stretch rate is inversely proportional to the flame radius for propagation spherical flames. Therefore, the small spherical flame kernel generated by energy deposition is highly stretched and its propagation speed depends strongly on the Markstein length which characterizes the variation in flame speed due to stretching [34]. Consequently, understanding the stretched flame propagation speed and Markstein length is helpful for examining the critical ignition condition. Here we first consider the freely propagating spherical flame without ignition energy deposition (i.e. $Q = 0$).

By solving Eqs. (4–6) numerically, we can obtain the change of flame propagation speed U with flame radius R at different levels of reaction reversibility. Consequently, the effects of reaction reversibility on unstretched/stretched flame speed and Markstein length can be assessed. In this study we fix the Zel'dovich number and temperature ratio (both are defined under the irreversible condition) to be $Z_{ad} = 10$ and $\sigma = 0.15$, respectively. Moreover, unity product Lewis number is assumed (i.e. $Le_P = 1.0$).

Figure 1 shows the normalized laminar flame speed and flame temperature of an adiabatic planar flame, which are similar to results reported by Daou [31]. As expected, the laminar flame speed and flame temperature both decrease with the reaction reversibility. The flame speed is observed to decrease much faster than the flame temperature. This is reasonable since the flame speed depends exponentially on flame temperature. Moreover, for unstretched planar flame, the flame temperature and laminar flame speed is nearly independent on fuel Lewis number.

In Fig. 1 a very broad range of reversibility parameter, $10^{-3} \leq \Gamma \leq 10^2$ is used. In the following, some specific value of Γ is used for the reversible case. It is difficult to model the practical chemistry by a simple reversible reaction of F $\Leftrightarrow$ Pwith some specific value of reversibility parameter Γ. Here we determine the value of reversibility parameter Γ based on the normalized adiabatic flame temperature shown in Fig. 1. For stoichiometric CO/air initially at 298 K and 1 atm., the adiabatic flame temperature for the irreversible case ($2CO + O_2 + 3.76N_2 = 2CO_2 + 3.76N_2$, assuming that the products only consist of CO_2 and N_2) is 2,663 K and that for the reversible case (assuming that the products consist of CO_2, CO, O_2, and N_2) is 2,400 K. Therefore, the normalized flame temperature for the reversible case is $T_b = (2{,}400 - 298)/(2{,}663 - 298) = 0.89$. According to the results (T_b versus Γ) shown in Fig. 1, this corresponds to $\Gamma = 0.3$. Similarly, for stoichiometric H_2/air with $2H_2 + O_2 + 3.76N_2 = 2H_2O + 3.76N_2$, we have $T_b = (2{,}430 - 298)/(2{,}519 - 298) = 0.96$ and hence $\Gamma = 0.1$. Therefore, we choose the value of $\Gamma = 0.2$ for the reversible case during the following analysis. The value of $\Gamma = 0.2$ is somewhat arbitrarily chosen. Nevertheless, the same conclusion can be drawn even when other values of Γ are used since the theory remains valid for all values of Γ.

Figure 2 shows the results for propagating spherical flame at different fuel Lewis numbers ($Le_F = 0.5$, 1.0, and 2.0) and reaction reversibility ($\Gamma = 0$ and 0.2). In Fig. 2, solutions on the horizontal axis with $U = 0$ denote flame balls, those close to the right vertical axis with $R = 1{,}000$ denote nearly planar flames, and those between them represent propagating spherical flames. For the irreversible case of $\Gamma = 0$, the

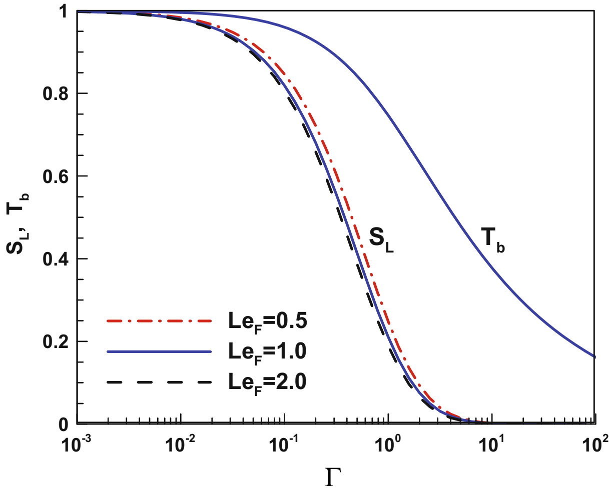

Fig. 1 Change of laminar flame speed and flame temperature of an adiabatic planar flame with reversibility parameter

results in Fig. 2 are the same as those for freely propagating spherical flame in [35]. The flame propagation speed and flame temperature are both greatly affected by the fuel Lewis number due to the coupling between positive stretch rate and preferential diffusion of fuel and heat [34]. When the reverse reaction is considered (i.e. $\Gamma = 0.2$), Fig. 2 shows that both the stretched flame speed and flame temperature are reduced. Therefore, similar to radiative heat loss, the endothermic reverse reaction, F $\leftarrow$ P, weakens the propagating spherical flame.

The change of the flame ball radius, R_Z, and flame ball temperature, T_Z, with fuel Lewis number, Le_F, are plotted in Fig. 3. The flame ball is purely controlled by diffusion and reaction. It is well known that R_Z increases with Le_F while T_Z decreases with Le_F (e.g. [4]). When there is reaction reversibility ($\Gamma = 0.2$), the flame ball temperature is reduced and its size becomes larger. Since the flame ball radius is the characteristic length scale that controls ignition for mixture with Lewis number below some critical value [11], the minimum ignition energy is expected to increase due to reaction reversibility. Moreover, Fig. 3 indicates that the influence of reversibility parameter on flame ball becomes weaker at larger fuel Lewis numbers. This is because the flame ball temperature quickly decreases with the fuel Lewis number ($T_Z = 1/Le_F$ for $\Gamma = 0$ [10]) and so does the reaction reversibility.

The spherical flame propagation is affected by the positive stretch rate of $K = 2U/R$. In Fig. 4 we plot the change of stretched flame speed with stretch rate. The unstretched flame speed (U at $K = 0$) is shown to be independent of fuel Lewis number for $\Gamma = 0$ while it decreases with Le_F for $\Gamma = 0.2$. This is consistent with results shown in Fig. 1. For $Le_F = 2.0$, nonlinear change of U with K is observed for $\Gamma = 0.2$ while nearly-linear behavior is shown for the irreversible case of $\Gamma = 0$. Therefore, reaction reversibility promotes the nonlinear effects of stretch on spherical flame propagation for large fuel Lewis number, which is an important issue in spherical flame method measuring the laminar flame speed and Markstein length [36,37].

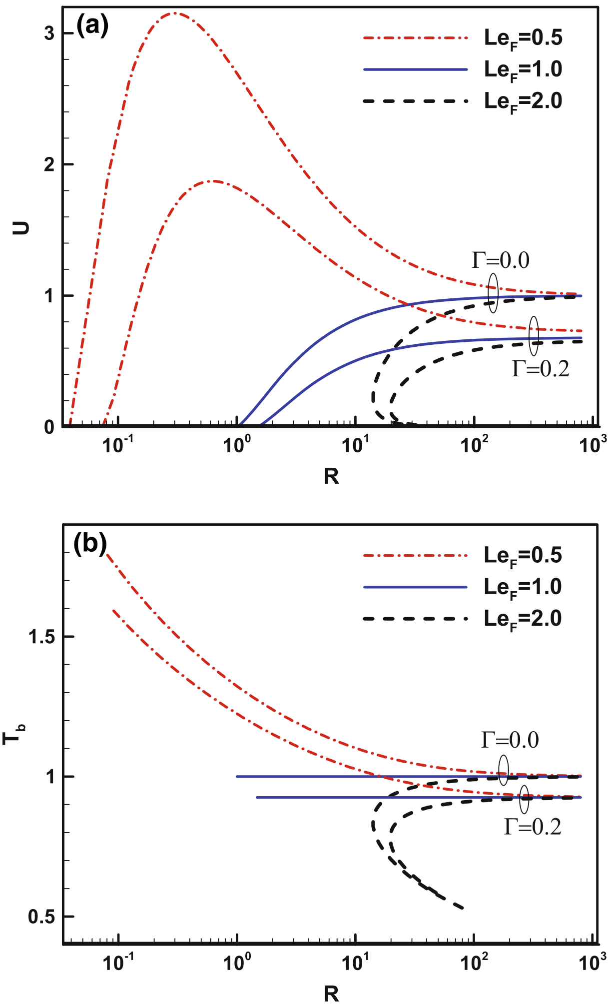

Fig. 2 Change of (**a**) flame propagation speed and (**b**) flame temperature with flame radius at different fuel Lewis numbers and reaction reversibility

For weakly stretched spherical flames, there is a linear relationship between the stretched flame speed, U, and stretch rate, K

$$U = U^0 - L \cdot K \tag{11}$$

where U^0 is the flame speed at zero stretch rate and L is the Markstein length (which is normalized by flame thickness). Therefore, the Markstein length is equal to the slope of the $U - K$ curve at $K \to 0$ in Fig. 4. Linear extrapolation is conducted to obtain the Markstein length and the results are plotted in Fig. 5. Figure 5a shows the dependence of Markstein length, L, on fuel Lewis number, Le_F, at $\Gamma = 0$ and $\Gamma = 0.2$. Compared to the irreversible case ($\Gamma = 0$), the positive Markstein length becomes larger while

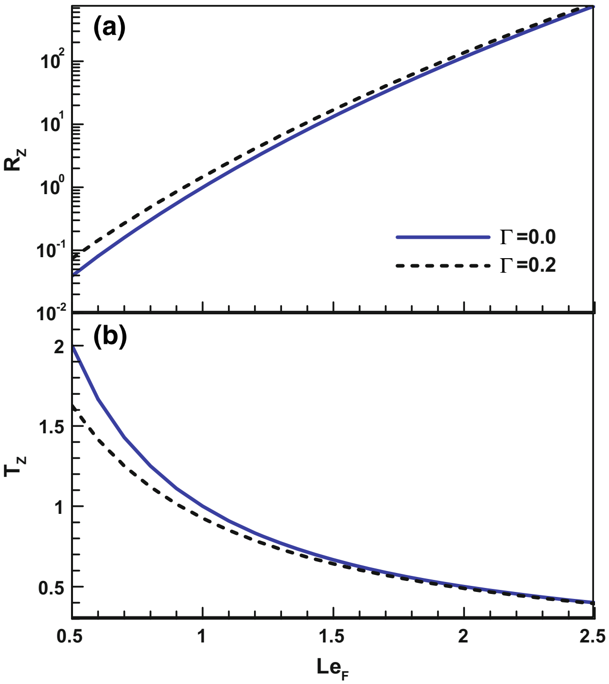

Fig. 3 Change of (**a**) flame ball radius and (**b**) flame ball temperature with fuel Lewis number

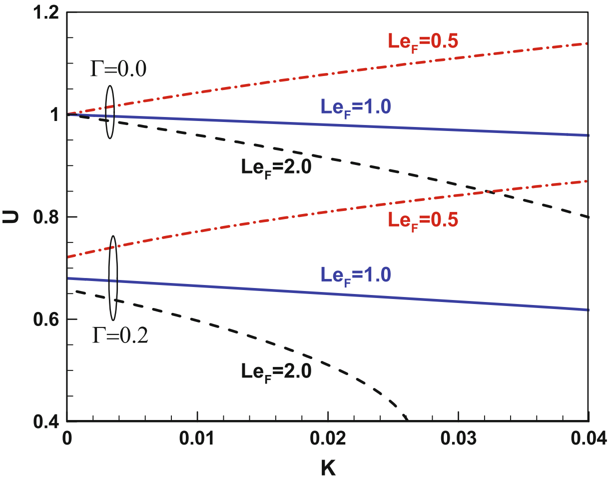

Fig. 4 Change of flame propagation speed with stretch rate at different fuel Lewis numbers and reaction reversibility

the negative one becomes smaller for the reversible case of $\Gamma = 0.2$. Therefore, the absolute value of Markstein length is enlarged by the reverse reaction, indicating that the influence of external stretching becomes stronger when the reverse reaction is

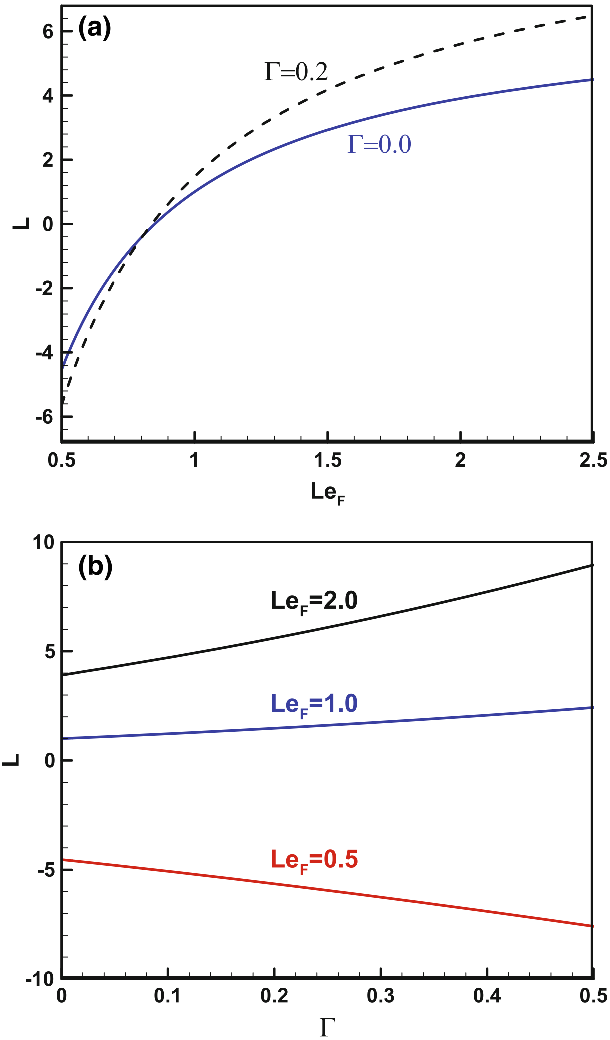

Fig. 5 Change of Markstein number with (**a**) fuel Lewis number and (**b**) reaction reversibility

considered. This is due to the facts that the endothermic reverse reaction makes the flame weaker and weaker flame is more sensitive to stretch rate [34]. The influence of reversible reaction is similar to that of radiative loss which also weakens the flame and increases the absolute value of Markstein length [38].

Figure 5b further demonstrates that with the increase of reaction reversibility, the absolute value of Markstein length increases and thereby the flame is more sensitive to the stretch rate. Both Fig. 5a, b shows that the influence of reaction reversibility on Markstein length is negligible for mixtures with Lewis number close to unity, and that the Markstein length is greatly affected by reaction reversibility for mixtures with Lewis number appreciably different from unity. Similar behavior was also observed

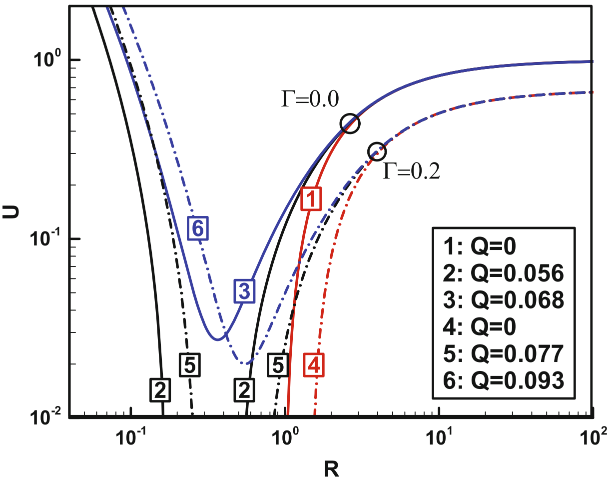

Fig. 6 Change of flame propagation speed with flame radius at different ignition powers for $Le_F = 1.0$ (*solid lines*, $\Gamma = 0$; *dash-dotted lines*, $\Gamma = 0.2$)

for the influence of radiative loss on Markstein length [38]. It is noted that though the influence of reaction reversibility on stretched counterflow flame was examined in [33], the dependence of Markstein length on reaction reversibility was not discussed therein. Besides, an explicit expression was derived for Markstein length that depends on heat loss intensity [38]. However, due to the strongly nonlinearity in Eqs. (4–6), here we cannot obtain an expression for Markstein length as a function of reaction reversibility in the limit of large flame radius. Nevertheless, Eqs. (4–6) can be readily solved numerically so that the Markstein length can be obtained at any value of reaction reversibility.

3.2 Effects of reaction reversibility on critical ignition condition

We now turn to the influence of reaction reversibility on spherical flame initiation. We consider the case with ignition power deposition at the center (i.e. $Q > 0$) and study the ignition kernel propagation with and without the reverse reaction.

The propagation speed of ignition kernel as a function of flame radius at different ignition powers and reaction reversibility are shown in Figs. 6 and 7 for $Le_F = 1.0$ and $Le_F = 2.0$, respectively. Figure 6 compares the results with and without the reversible reaction (solid lines, $\Gamma = 0$; dash-dotted lines, $\Gamma = 0.2$). When there is no ignition power deposition at the center (i.e. $Q = 0$), the results are the same as those in Fig. 2a and the outwardly propagating spherical flame only exists when its radius is larger than the flame ball radius ($R_Z = 1$ for $\Gamma = 0$ and $R_Z = 1.47$ for $\Gamma = 0.2$). When a small external power is deposited at the center (lines 2 and 5 in Fig. 6), there exist two branches of solutions: the original traveling flame branch on the right and a new ignition kernel branch on the left. Consequently, there are two flame ball solutions whose radii are denoted by R_Z^- and R_Z^+. The difference, $R_Z^+ - R_Z^-$, decreases with the

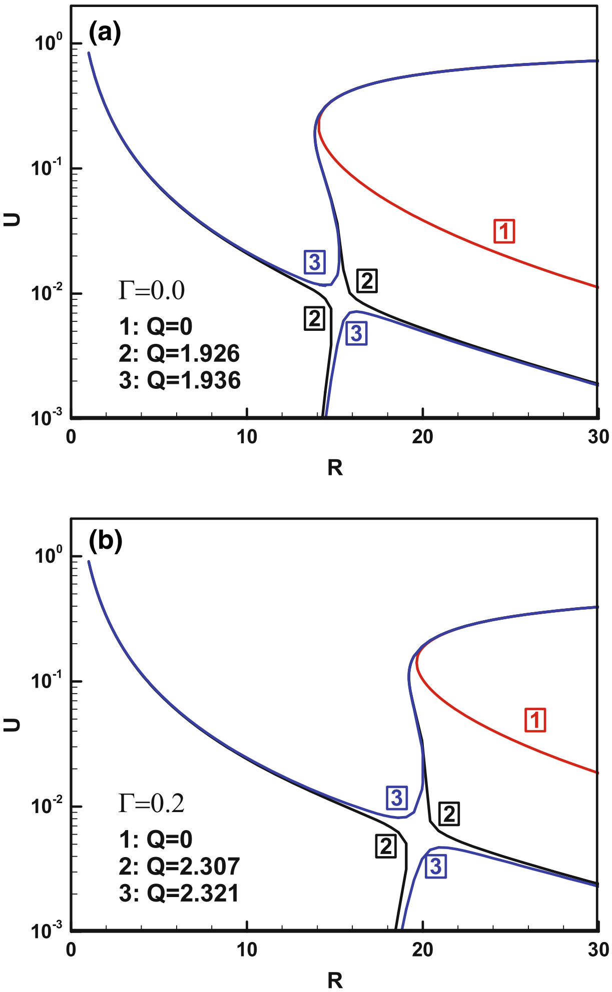

Fig. 7 Change of flame propagation speed with flame radius at different ignition powers for $Le_F = 2.0$: (**a**), $\Gamma = 0$; (**b**), $\Gamma = 0.2$

ignition power. When the external power is larger than the minimum ignition power, the left ignition kernel branch merges with the right traveling flame branch and no flame ball solution exists, indicating that successful ignition is achieved [4,11,16]. Therefore, the minimum ignition power, denoted by Q_C, is reached when $R_Z^+ = R_Z^-$ which is called the critical ignition radius (denoted by R_C) [11]. For the irreversible case of $\Gamma = 0$, we have $Q_C = 0.062$ and $R_C = 0.36$. When the reverse reaction is considered ($\Gamma = 0.2$), the critical ignition conditions become $Q_C = 0.085$ and $R_C = 0.56$. Therefore, the minimum ignition power and critical ignition radius are both greatly increased by the reverse reaction.

Figure 7 shows the results for $Le_F = 2.0$. For $Q = 0$, a C-shaped U–R branch is observed (line 1 in Fig. 7). When the ignition power is introduced (lines 2 in Fig. 7),

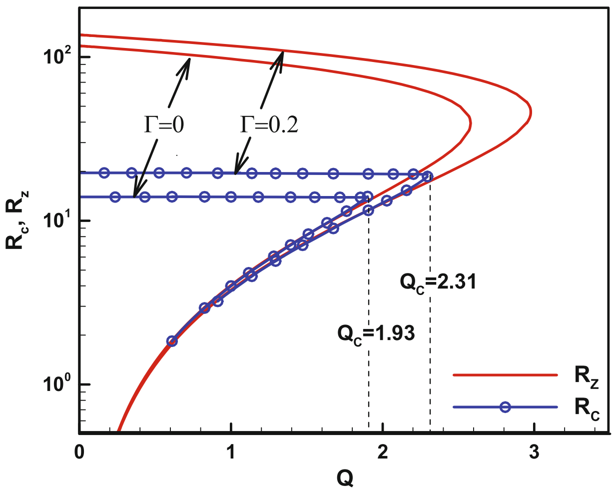

Fig. 8 Change of upper and lower critical flame radii and flame ball radii with ignition power for $Le_F = 2.0$

an ignition-kernel branch appears on the left with a turning point corresponding to the maximum possible flame radius. The radii at the left and right turning points are respectively defined as the lower and upper critical flame radii, which are denoted by R_C^- and R_C^+. Unlike the case of $Le_F = 1.0$ for which critical ignition occurs when $R_Z^- = R_Z^+$, the critical ignition condition for $Le_F = 2.0$ is reached when $R_C^- = R_C^+$. This is because the ignition process is greatly affected by the fuel Lewis number (see more details in Ref. [11]). Comparison between Figs. 7a, b indicates that reaction reversibility does not qualitatively affect the ignition process. Nevertheless, the minimum ignition power and critical ignition radius are both enlarged by the reverse reaction. This is further demonstrated in Fig. 8 which shows the change of lower and upper critical flame radii as well as the flame ball radius with the ignition power. The minimum ignition power is reached when $R_C^+ = R_C^-$ and is denoted by the dashed line in Fig. 8. According to the values shown in Fig. 8, the minimum ignition power and critical ignition radius are respectively increased by 20 and 48 % after changing the reversibility parameter from $\Gamma = 0$ to $\Gamma = 0.2$. As mentioned before, the present results on ignition reduce to those in previous studies [4,11,16] when the reversibility parameter is zero ($\Gamma = 0$).

Figure 9a compares the critical ignition conditions for $\Gamma = 0.2$ with those for $\Gamma = 0$ in a broad range of fuel Lewis number, $0.5 \leq Le_F \leq 2.0$. The minimum ignition power is shown to be increased by 20–50 % and the critical ignition radius by 40–70 % after changing the reversibility parameter from $\Gamma = 0$ to $\Gamma = 0.2$. Moreover, the normalized minimum ignition power and critical ignition radius are both shown to decrease with fuel Lewis number. This is due to the facts that the temperature of stretched spherical flame decreases with fuel Lewis number (see Fig. 2) and that the reaction reversibility increases with temperature. This trend is opposite to that for heat loss: when heat loss is considered, the normalized minimum ignition power and critical ignition radius both increase with fuel Lewis number (see Fig. 11 in Ref. [10]).

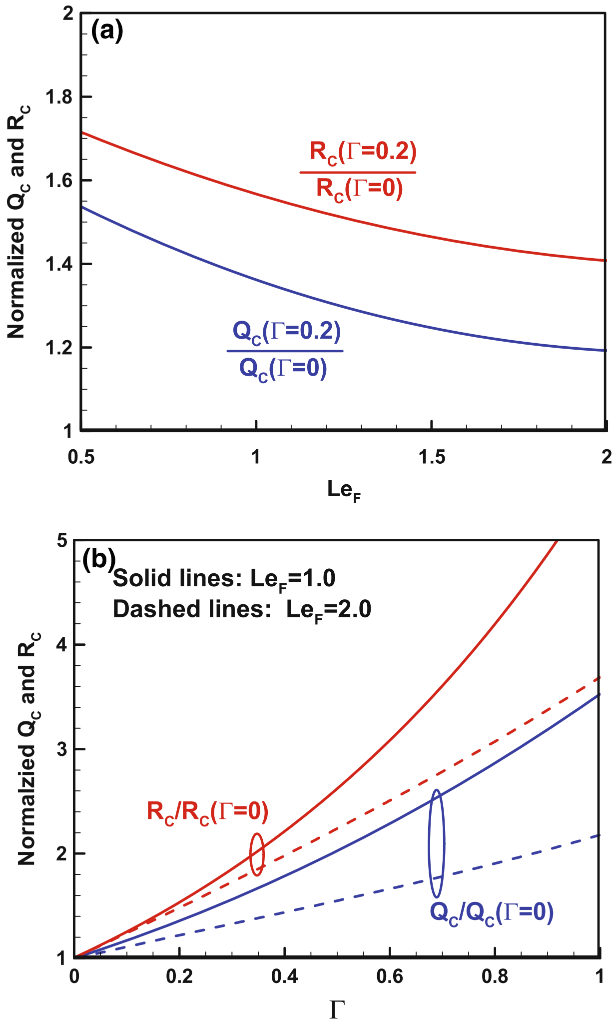

Fig. 9 Change of normalized minimum ignition power and critical ignition radius with (**a**) fuel Lewis number and (**b**) reaction reversibility

Figure 9b shows the change of the normalized minimum ignition power and critical ignition radius with the reaction reversibility for $Le_F = 1.0$ and $Le_F = 2.0$. It is observed that both Q_C and R_C increase monotonically with the reversibility parameter Γ and that the influence of reaction reversibility for $Le_F = 1.0$ is greater than that for $Le_F = 2.0$, which is consistent with results in Fig. 9a.

4 Conclusions

A theoretical model for spherical flame initiation and propagation with a single reversible reaction is developed in this study. The present model extends previous studies [7,10] on spherical flame initiation and propagation beyond the traditional framework of one-step irreversible reaction. Large-activation-energy asymptotic analysis is conducted and analytical correlations describing spherical flame initiation and propagation are derived. Based on these correlations, the effects of reaction reversibility on propagating spherical flame, flame ball, and critical ignition condition are assessed. It is found that the spherical flame propagation speed is reduced while the absolute value of Markstein length is enlarged by the reaction reversibility. Therefore, the influence of external stretching on stretched flame speed becomes stronger when the reverse reaction is considered and this is similar to the effects of heat loss. For the ignition process, the reaction reversibility does not qualitatively affect the development of ignition kernel. Nevertheless, the minimum ignition power and critical ignition radius are both enlarged by the reverse reaction. Furthermore, unlike that of heat loss, the influence of reversibility parameter on minimum ignition power and critical ignition radius is found to decrease with fuel Lewis number. This is because when the fuel Lewis number increases, the flame temperature of positively stretched flame decreases and so does the reaction reversibility.

Acknowledgments This work was supported by National Natural Science Foundation of China (Nos. 51322602 and 51136005), Doctoral Fund of Ministry of Education of China (No. 20120001110080), and State Key Laboratory of Engines at Tianjin University (No. K2012-02).

References

1. B. Lewis, G. Von Elbe, *Combustion Flames and Explosive of Gases*, 2nd edn. (Academic Press, New York, 1961)
2. F.A. Williams, *Combustion Theory*, 2nd edn. (Benjamin-Cummins, Menlo Park, 1985)
3. Y.B. Zeldovich, *The Mathematical Theory of Combustion and Explosions* (Consultants Bureau, New York, 1985)
4. B. Deshaies, G. Joulin, Combust. Sci. Technol. **37**, 99 (1984)
5. M.L. Frankel, G.I. Sivashinsky, Combust. Sci. Technol. **31**, 131 (1983)
6. P.D. Ronney, G.I. Sivashinsky, SIAM J. Appl. Math. **49**, 1029 (1989)
7. L.T. He, Combust. Theory Model. **4**, 159 (2000)
8. M. Matalon, C. Cui, J.K. Bechtold, J. Fluid Mech. **487**, 179 (2003)
9. J.K. Bechtold, C. Cui, M. Matalon, Proc. Combust. Inst. **30**, 177 (2005)
10. Z. Chen, Y. Ju, Combust. Theory Model. **11**, 427 (2007)
11. Z. Chen, M.P. Burke, Y. Ju, Proc. Combust. Inst. **33**, 1219 (2011)
12. U. Maas, J. Warnatz, Combust. Flame **74**, 53 (1988)
13. A. Frendi, M. Sibulkin, Combust. Sci. Technol. **73**, 395 (1990)
14. H.J. Kim, S.H. Chung, C.H. Sohn, KSME Int. J. **18**, 838 (2004)
15. W.K. Zhang, Z. Chen, W.J. Kong, Combust. Flame **159**, 151 (2012)
16. M. Champion, B. Deshaies, G. Joulin, K. Kinoshita, Combust. Flame **65**, 319 (1986)
17. Y. Ko, R.W. Anderson, V.S. Arpaci, Combust. Flame **83**, 75 (1991)
18. A.P. Kelley, G. Jomaas, C.K. Law, Combust. Flame **156**, 1006 (2009)
19. P.D. Ronney, Opt. Eng. **33**, 510 (1994)
20. H. Zhang, Z. Chen, Combust. Flame **158**, 1520 (2011)
21. H. Zhang, P. Guo, Z. Chen, Proc. Combust. Inst. **34**, 3267 (2013)
22. J.W. Dold, Combust. Theory Model. **11**, 909 (2007)
23. V.V. Gubernov, H.S. Sidhu, G. Mercer, A.V. Kolobov, A.A. Polezhaev, J. Math. Chem. **44**, 816 (2008)
24. G.J. Sharpe, Combust. Theory Model. **12**, 717 (2008)
25. V. Gubernov, A.V. Kolobov, A.A. Polezhaev, H.S. Sidhu, G. Mercer, Proc. R Soc. A **466**, 2747 (2010)
26. V.V. Gubernov, A.V. Kolobov, A.A. Polezhaev, H.S. Sidhu, Combust. Theory Model. **15**, 385 (2011)
27. G.J. Sharpe, S.A.E.G. Falle, Combust. Flame **158**, 925 (2011)

28. V.V. Gubernov, A.V. Kolobov, A.A. Polezhaev, H.S. Sidhu, Combust. Flame **160**, 1060 (2013)
29. V.N. Kurdyumov, D. Fernandez-Galisteo, Combust. Flame **159**, 3110 (2012)
30. H. Zhang, Z. Chen, Combust. Theory Model. **17**, 682 (2013)
31. J. Daou, Combust. Theory Model. **12**, 349 (2008)
32. J. Daou, Combust. Theory Model. **13**, 189 (2009)
33. J. Daou, Combust. Theory Model. **15**, 437 (2011)
34. C.K. Law, *Combustion Physics* (Cambridge University Press, Cambridge, 2006)
35. Y. Wu, Z. Chen, Acta Mech. Sin. **28**, 359 (2012)
36. Z. Chen, Combust. Flame **158**, 291 (2011)
37. A.P. Kelley, C.K. Law, Combust. Flame **156**, 1844 (2009)
38. Z. Chen, X. Gou, Y. Ju, Combust. Sci. Technol. **182**, 124 (2010)